Journal of Thermal Analysis and Calorimetry, Vol. 93 (2008) 1, 19–26

THERMOANALYTICAL AND MORPHOLOGICAL STUDIES OF CROSS-LINKED LATEX FILMS BY ADVANCED TECHNIQUES

R. Joshi[1,2], *E. Lefevre*[1,2], *C. Patel*[1,2], *T. Provder*[3*], *R. Crombez*[1,4], *W. Shen*[1,4] *and F. Jones*[1,2]

[1]Coatings Research Institute, Eastern Michigan University, Ypsilantio, MI 48197, USA
[2]School of Engineering Technology, Eastern Michigan University, Ypsilanto, MI 48197, USA
[3]Polymer and Coatings Consultants, LLC; 26567 Bayfair Dr., Olmsted Falls, OH 44138, USA
[4]Department of Physics Eastern Michigan University, Ypsilanto, MI 48197, USA

In the present report, thermal analysis (TMDSC, DMA, TG, stress–strain analysis), nano-indentation and AFM morphological characterization of cross-linkable latexes, prepared with either a pre-coalescence cross-linker (1,3–butylene glycol dimethacrylate) or post-coalescence cross-linker (adipic dihydrazide) at various levels of cross-linking, were done. The study assesses the effect of type and level of cross-linking on the film formation process through the evolution of mechanical properties and latex morphology. In addition, the final fundamental thermal and mechanical properties, specific end-use properties and latex morphology resulting from the film formation process are reported.

Keywords: *AFM, DMA, morphology, nano-indentation, pre-coalescence cross-linking, post-coalescence crosslinking, stress-strain properties*

Introduction

In 1978 Bufkin and Grawe [1–5] published a series of review articles on cross-linking latexes with several thousands references. These articles provided an extensive overview of the various cross-linking chemistries available before 1978. Many thousands of patents and publications on cross-linkable latexes have appeared since then. For examples of recent publications [6–14] and patents [15–18]. In 2004, Winnik and Taylor [6] published a fundamental review paper covering advancements in cross-linking technology, various cross-linking chemistries and a masterful overview on their film formation mechanisms. Surprisingly few, if any, of the thousands of publications contain systematic comparisons of film properties of 'pre-coalescence' (internal) and 'post-coalescence' (external) cross-linked latexes, the subject of this paper.

By 'pre-coalescence cross-linked latexes' we mean latexes that are prepared by emulsion polymerization of conventional monomers such as mono-acrylates, mono-methacrylates or styrene in combination with di- or poly-functional monomers such as di-methacrylates or divinyl benzene which cause a degree of cross-linking within the latex particles. It is sometimes called 'intraparticle crosslinking'. The cross-linking reaction takes place before the coalescence of particles. In this study, we used 1,3-butylene glycol dimethacrylate (1,3-BGDMA) as the pre-coalescence cross-linker.

By 'post-coalescence cross-linked latexes' we mean latexes that are prepared with reactive sites such as hydroxyl groups and are cross-linked during film formation by a cross-linker that is added to the coating formulation but not co-polymerized in the latex. Another term is 'interparticle crosslinking'.

Many combinations of reactive sites and cross-linkers have been described in literature [6]. In this study we used diacetone acrylamide (DAA) as the monomer to place reactive sites within the latex and adipic dihydrazide (ADDH) as the post-coalescence cross-linker. This combination of site and cross-linker has been described in trade literature [13] and in numerous patents [15–18] and is being utilized by some major coatings and ink companies.

Experimental

Materials

Here we report the study of comparable latexes containing 0–4 mass% of pre-coalescence cross-linker (1,3-BGDMA) and 0–5 mass% of reactive monomer for post-coalescence cross-linker (DAA). Both the pre-coalescence and post-coalescence latex series were prepared by semi-continuous emulsion polymerization using target glass transition temperatures (T_g) of 7 and 22°C. The latexes are coded I for pre-coalescence or internal, E for post-coalescence or external, L for low

* Author for correspondence: tprovder@cox.net

1388–6150/$20.00

Akadémiai Kiadó, Budapest, Hungary
Springer, Dordrecht, The Netherlands

T_g, H for high T_g and a number for the mass% of cross-linker or reactive site in the monomer line up. Thus, for example, IL-2 means an internally (or pre-coalescence) cross-linked, low T_g latex with 2.0 mass% of 1,3-BGDMA and EH-1 means an externally (or post-coalescence) cross-linked, high T_g latex with 1.0 mass% of DAA.

The resulting latexes have, % non-volatile matter (%NVM) ranging from 46–47%, average particle size ranging from 0.11–0.13 μm and pH values ranging from 9.1–9.9. The films cast from these latexes were characterized using advanced instruments described in experimental section.

Methods

Measurements with DMA and MSDC

For glass transition temperature (T_g) measurement specimens were prepared on glass panels by drawing the latexes down using a square wet film applicator (Paul N. Gardner Co., Inc.) with 0.25 mm (wet) clearance on glass panels. The panels were dried in an oven at 55°C and 50% relative humidity (RH) for 10–12 h. The films were then stored at ambient conditions for a week before testing. The T_g of the dried films were determined by TA instrument-TA 2920 Temperature Modulated Differential Scanning Calorimetry (TMDSC) with liquid nitrogen cooling system (LNCS) accessory under nitrogen purge at flow rate of 50 mL min^{-1}. For testing, the samples were kept in closed aluminum non-hermetic pans. Temperature scans were done from –100 to 100°C at 2°C min^{-1} with modulation of ±1.00°C at every 60 s under nitrogen. The MDSC equilibrated at –100°C for 5 min.

Dynamic mechanical analyses (DMA) were conducted using TA Instruments Model Q800 Dynamic Mechanical Analyzer (DMA) with LNCS accessory. Specimens for stress–strain and dynamic mechanical studies were prepared on glass panels as described in TMDSC studies section. A film cutter (supplied by TA instruments) was used to cut, at constant depth, rectangular specimens about 15–20 mm long, 3–6 mm wide and 0.1–0.2 mm thick from the cured films. Two sets of studies were performed – (1) on the 1st day (at the end of the cure into the oven) and (2) on the 7th day (7 days after being kept at ambient conditions). Thermogravimetric analysis (TG) of latex films were run to establish the onset temperature for degradation so DMA analyses did not exceed this temperature.

The stress–strain studies were done at the room temperature in air on the Q800 DMA with the thin film tension clamp. DMA measurements of dried specimen were done at 1 Hz with a thin film tension clamp over the temperature range of –100 to 100°C, using liquid nitrogen as a coolant. The flow rate of liquid nitrogen into the DMA depends upon the starting temperature desired and is controlled by the ramp rate or heating rate of 3°C min^{-1}.

Measurements with the nanoindenter

The nanoindentation or nanoscratch tester used in this study was a computer controlled 'Nanoindenter XP', made by MTS Systems Corporation. Its operation was described in detail in a previous paper by Shen *et al*. [19]. In the present study, a Berkovich diamond tip with an angle of 142.4° was used for the indentation experiments. The tests were performed by applying Z-direction force (loading) at a constantly increasing rate for 15 s, holding at maximum force for 30 s and decreasing the force to zero (unloading) during 15 s. The holding time was 30 s. Temperature was 26–28°C. The maximum force applied during loading and unloading was varied depending on the hardness of particular specimens. The instrument automatically plots a curve showing the depth of penetration of the tip into the material *vs*. force applied during loading, holding and unloading. Usually, the tip continues to move into the surface during the holding stage as a result of viscous creep of the material. Also, usually, the unloading curve does not coincide with the loading curve, reflecting a residual plastic deformation. The instrument automatically calculates hardness (H) and elastic modulus (E). The interpretation of H and E values measured this way was discussed in a previous paper by Shen *et al*. [19].

Measurements with atomic force microscope

An atomic force microscope (NanoScope III, Digital Instruments) was used to observe surface morphology through friction mode images. The contact mode was used to capture the friction force images of samples. Both surface morphology and friction force images were captured at image sizes of 2 μm×2 μm and 5 μm×5 μm. For every sample, two sets of images were captured.

Results and discussion

TMDSC results

TMDSC analysis of interphases in multi-component materials including latex has been reported by Song *et al*. [20]. TMDSC profiles were obtained for all cross-linked latex samples. The TMDSC analysis showed that in case of pre-coalescence cross-linked latexes addition of up to 4 mass% of 1,3-BGDMA has significant effect on T_g that the T_g is increased at the 4% level. In case of post-coalescence latexes there is a negligible effect on the T_g at the 5% level. Table 1

Table 1 TMDSC T_g (°C) and theoretical Fox T_g (°C) of EL, IL, EH and IH series

Samples	TMDSC T_g/°C	Fox T_g/°C	Samples	TMDSC T_g/°C	Fox T_g/°C
EL-0	6	2.72	EH-0	24	13.66
EL-1	9		EH-1	25	
EL-2	7		EH-2	25	
EL-5	5		EH-5	23	
IL-0	6	2.72	IH-0	24	13.66
IL-0.25	8		IH-0.25	25	
IL-0.6	5		IH-0.6	25	
IL-1.2	6		IH-1.2	24	
IL-2	5		IH-2	25	
IL-4	13		IH-4	33	

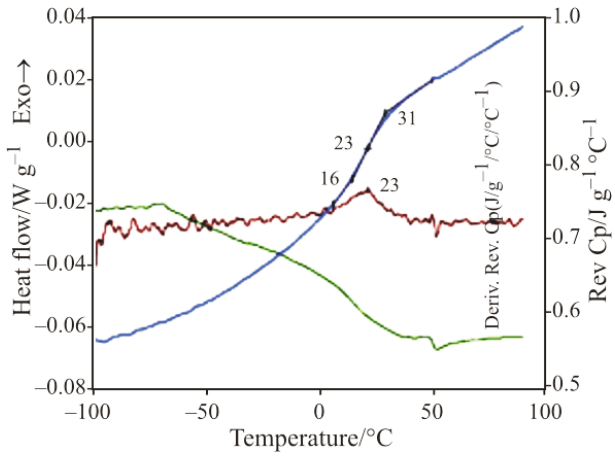

Fig. 1 TMDSC analysis of EH-5 sample

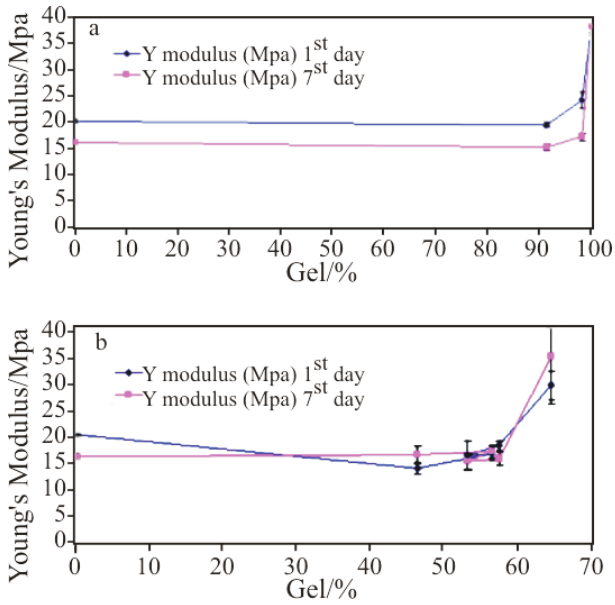

Fig. 2 Representative curves showing 1st day *vs.* 7th day comparison of stress–strain analysis of a – EL and b – IL series

shows respective values of TMDSC T_g (°C) for all samples. Figure 1 shows a representative TMDSC profile for EH-5 displaying the total heat flow, reverse (rev.) heat capacity (C_p) and derivative rev. C_p curves.

DMA results

DMA and stress–strain analysis of free films of acrylic emulsion paints has been reported by Ormsby *et al.* [21, 22]. The liquid coating formulations were synthesized and coated on glass panels and cured at 55°C and 50% relative humidity (RH) for 10–12 h before measurements were made. Two sets of studies were performed: (1) on the first day (at the end of overnight cure into the oven) and (2) on the 7th day (7 days of ambient cure after overnight cure into the oven). Comparison between the 1st day studies and the 7th day studies were done. Figure 2 shows Young's modulus *vs.* %gel of EL and IL samples of 1st *vs.* 7th day studies. Figure 3 shows representative tan delta curves of EL-2 and IL-1.2 samples of 1st *vs.* 7th day studies. The comparison showed that similar trend is observed when comparing the results obtained in 1st and 7th day for stress–strain results and dynamic mechanical analysis. The values are

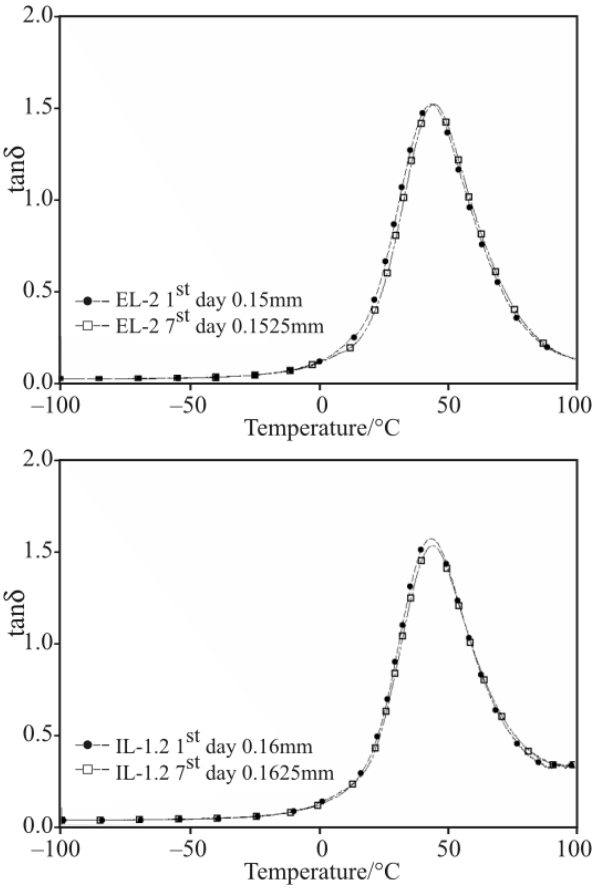

Fig. 3 Representative tan delta curves showing 1st day *vs.* 7th day comparison of DMA studies of a – EL-2 and b – IL-1.2 samples

not the same but are very close (within the experimental error or standard deviations and the curves show the same inflection.

Corroboration of stress–strain and nano-indentation analysis

Corroboration of the average stress–strain curves, where each curve represents an average of 5–6 replicates and the nano-indentation analyses were done. Such corroboration gives important information about fundamental mechanical properties of materials.

With increasing levels of post-coalescence or external cross-linking, Young's modulus increases as expected. However, a significant decrease in area under the curve and strain at break is observed. The sample becomes more brittle. Going from 0 to 1% cross-linker shows hardly any difference in Young's modulus. However, from 0% cross-linking to 5% of cross-linking Young's modulus values go from approximately 20 to 38 MPa. This has also been observed by nano-indentation characterization which shows, that the elastic modulus values for 0 and 1% remains almost similar while there has been a significant build up in modulus value going from 0 to 5% cross-linking. Although, it should be noted that nano-indentation gives a surface modulus value while stress–strain characterization gives a bulk modulus value. Figures 4 and 5 show hardness and modulus values from nano-indentation analysis of EL, EH, IH and IL samples.

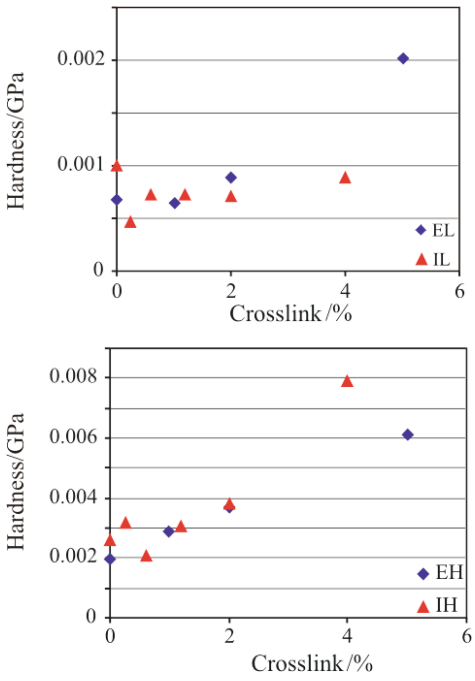

Fig. 4 Comparison of hardness of samples in groups EL, IL and EH, IH with different cross-linker levels. Test force=1 mN

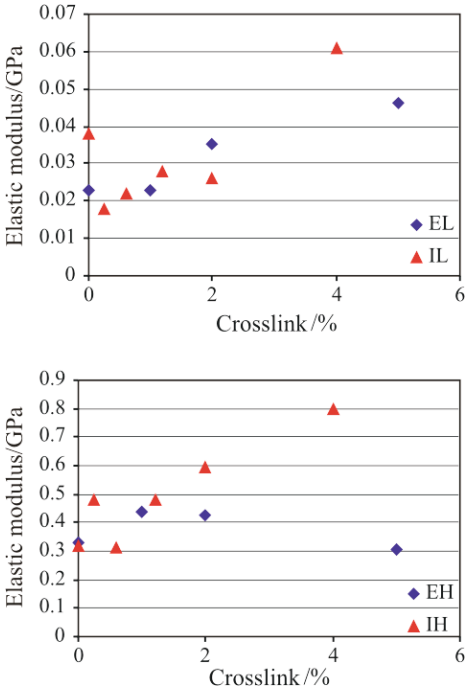

Fig. 5 Comparison of elastic modulus of samples in groups EL, IL and EH, IH with different cross-linker levels. Test force=1 mN

For post-coalescence cross-linked high T_g latexes the modulus values increase with the level of cross-linking and the sample becomes more brittle. The modulus values are higher than the low T_g counterparts, showing the effect of high glass transition temperature with cross-linking. In contrast to low T_g samples, the high T_g samples shows a significant change in modulus value as cross-linking level goes from 0 to 1%. Both stress–strain and nano-indenter data at 1 and 2% show a similar build up in modulus value compared to 0% cross-linking. However, in nano-indentation test, samples with 5% cross-linker shows significant drop in elastic modulus in contrast to Young's modulus by stress–strain. This difference may reflect the different measurement methods.

In the case of pre-coalescence cross-linking, as the level of cross-linking increases interdiffusion of particles is retarded by cross-linking. It is observed that between 0.25 to 2% cross-linker, the modulus value is comparatively lower than 0% cross-linking. At 5% of cross-linking the samples builds up the modulus value but becomes brittle. The same trend is observed with nano-indenter data where it is evident that 0% cross-linking has higher modulus value than modulus values at 0.25 to 2%. However, at highest level of cross-linking the modulus value is the highest. At high T_g in pre-coalescence cross-linked latexes from 0–1.2% cross-linker, the modulus value increases. However, the modulus value decreases at 2% but significantly increases at 4%. The drop in modulus value at 2% could be due to retarded interdiffusion of

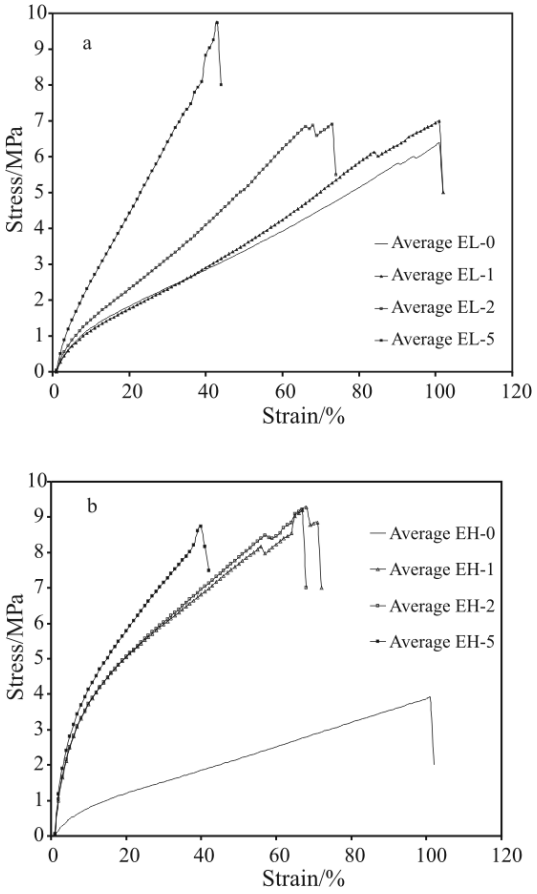

Fig. 6 Representative average stress–strain curves of a – EL and b – EH series

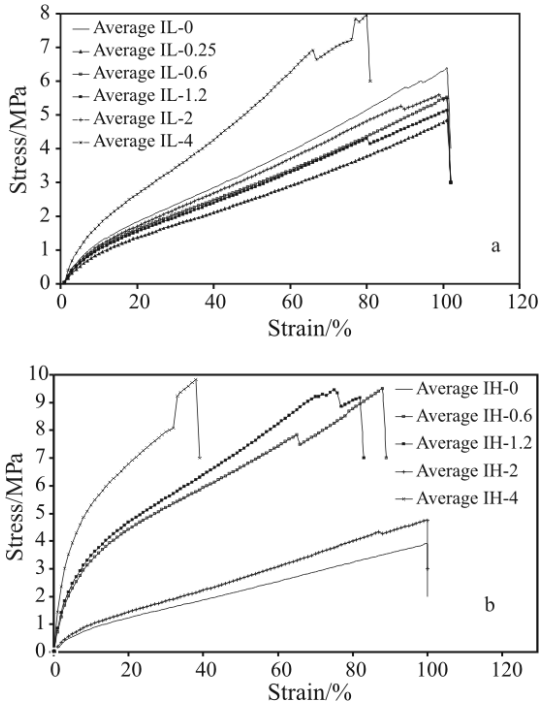

Fig. 7 Representative average stress–strain curves of a– IL and b– IH series

polymer chains between particles. At 4% the increase in modulus may be due to significantly increasing intra-particle cross-linking without further interrupting interdiffusion of polymer chains compared to 2%. Figures 6 and 7 show representative average stress–strain curves of EL, EH, IH and IL series.

Dynamic mechanical properties

Dynamic mechanical characterization of heterogeneous polymers is dependent not only on the chemical composition of a material but also on physical or structural arrangement of the phases in a bulk polymer. DMA analysis gives an insight into intrinsic mechanical properties of a polymer. Figure 8 shows representative DMA temperature scan graphs of the post-coalescence cross-linked latexes for low T_g and high T_g samples.

DMA provides information about the viscoelastic properties (storage modulus and loss modulus) of a polymer as a function of frequency and temperature. The inflection point of storage modulus is related to T_g of the polymer. The tan delta curve is calculated as ratio of the loss modulus and storage modulus. The

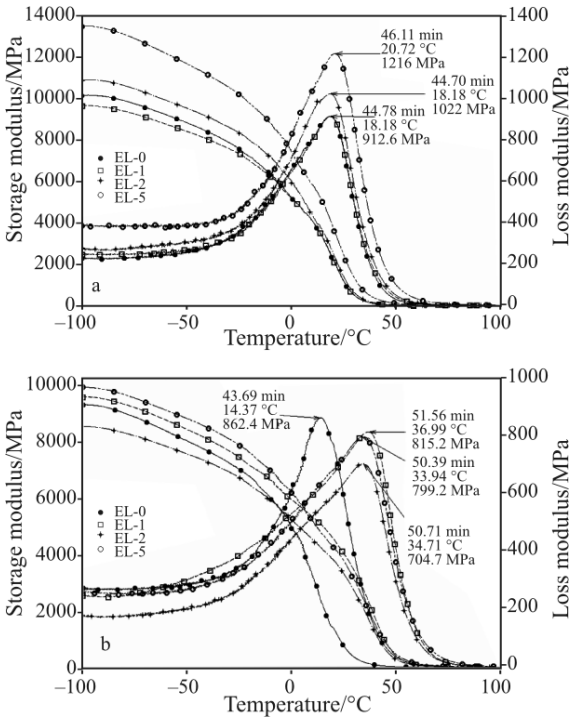

Fig. 8 Storage and loss modulus curves of post-coalescence cross-linked latexes: low and high T_g a – EL and b – EH series

point where the storage modulus curve flattens is indicator of rubber plateau. For these latex samples, rubbery plateau values are essentially close to zero for the storage modulus.

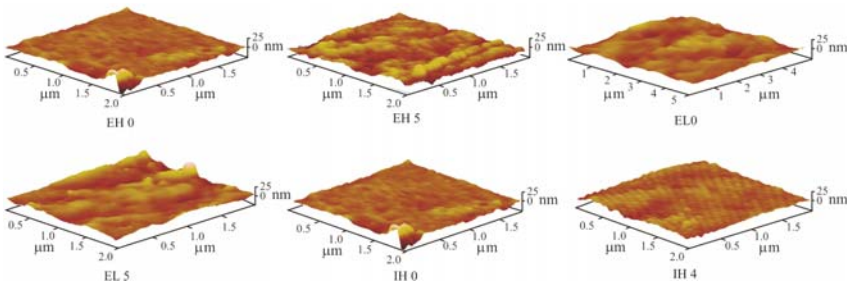

Fig. 9 Conditioned sample AFM friction images of cross-linked latexes

Atomic force microscopy (AFM) results

AFM contact mode friction images of representative samples dried in an oven at 55°C and 50% RH for 10–12 h are shown in Fig. 9. Comparing the images of low T_g samples and high T_g samples show the effect of T_g on film formation. Also, AFM images of surfaces of the films cast from latexes EL-5 and IH-4 shows surface peaks and valleys with lateral dimensions of the same order of magnitude as the original latex particles, as commonly observed with films cast from latexes. Note that the height of the peaks at the surface of the EL-5 film is an order of magnitude larger than the height of the peaks in the IH-4 film. This observation suggests that the rate of the cross-linking reaction was fast enough to significantly retard the homogenization of the film, at least near the surface.

Time evolution of morphology by AFM

Figure 10 shows morphological changes observed by AFM contact mode friction images during the film

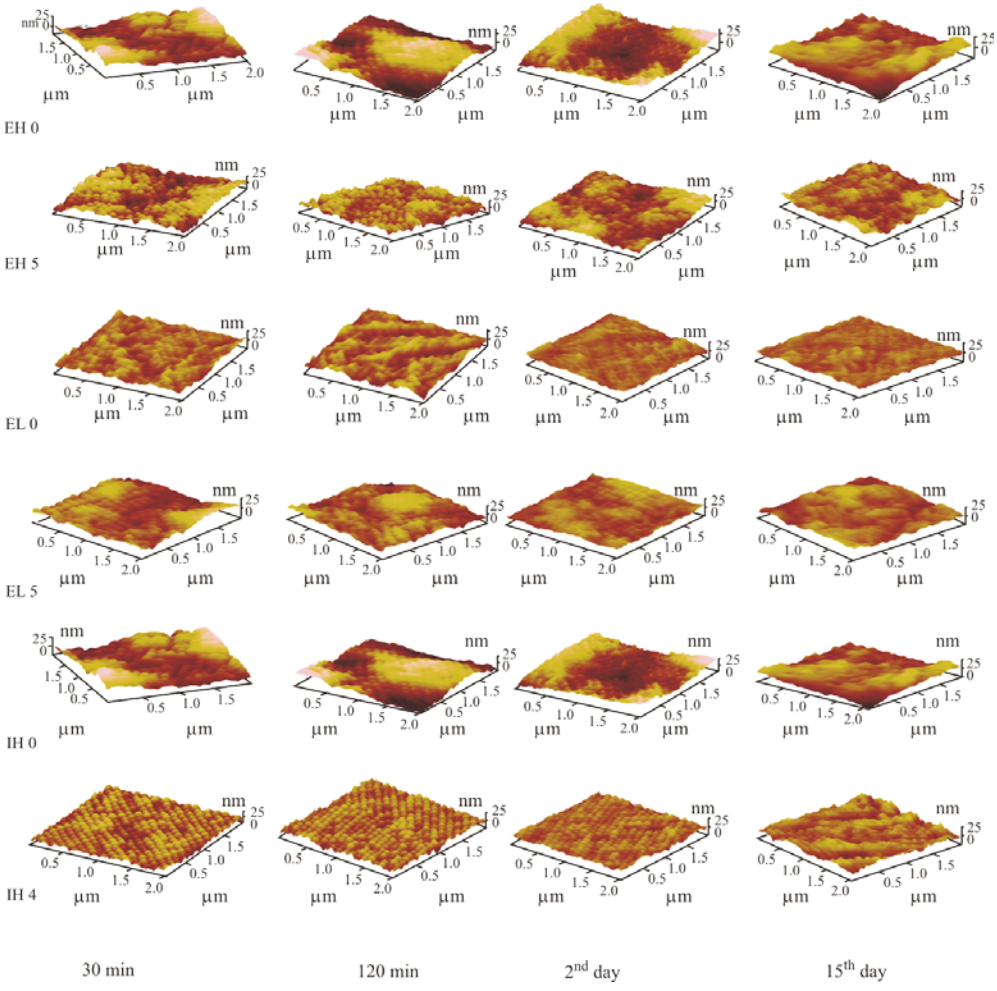

Fig. 10 Representative friction images of morphological changes observed by AFM contact mode during the film formation

formation. The latex films were applied at room temperature and film formation was studied at regular time-intervals. A useful model of film formation by latexes [6–9] involves three major, overlapping, stages.

The third stage, of film formation, involves interdiffusion of polymer chains from different latex polymers. Interdiffusion knits vestigal particles together and is essential if the polymer film is to realize the mechanical properties of which its composition is capable. Complete interdiffusion is not necessary, however; it is only necessary for the molecules from adjacent particles to interpenetrate to a distance comparable to the root-mean-square radius of gyration (R_G) the individual molecules [9], typically a smaller distance than the diameters of the original latex particles.

The film formation process as a function of time is clearly evident in AFM images shown in Fig. 10. The effect of T_g on film formation can be clearly seen when the images of EL-5 and EH-5 are compared. The EL-5 films appear smooth and homogenous compared to EH-5 at similar time intervals. The effect of level of cross-linking can also be seen when the images of EH-0 and EH-5 are compared. Looking at EH-5 images latex particles interdiffusion can be clearly observed. The rate of cross-linking here certainly affect of rate of interdiffusion of particles. Also, effect of type of cross-linking can also be seen when comparing the film formation images of EL-5 and IH-4. The image of EL-5 shows more homogenous structure when compared to IH-4 images at similar time intervals.

Time-evolution of mechanical properties

The liquid coatings sample were applied and cured on glass panels at room temperature. The stress–strain and DMA analysis of samples of dried coatings at specified time intervals from 1st day to 10th day were done. Figure 11 shows representative stress–strain average curves and storage and loss modulus curves of sample EH-0. The graph shows clear evidence of build up in mechanical properties as a function of time. Going from the first day to second day to fifth day the mechanical properties show significant build up. Such study will yield interesting corroboration of DMA properties with the AFM morphological properties.

Future goals

In future we aim to implement appropriate mixture design experiments utilizing pre-coalescence and post-coalescence cross-linkable latexes to obtain optimum end-use properties. Also, we intend to corroborate the AFM time-based study with Adaptive Speckle Image

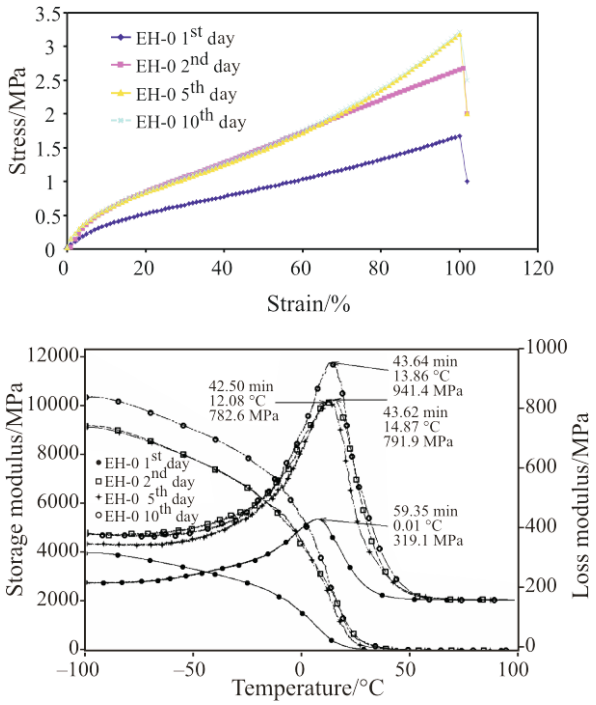

Fig. 11 Time based stress–strain and DMA analysis of EH-0 at ambient conditions

Interferometry (ASII) Drying Curves and evolution of fundamental mechanical properties by DMA. To design, synthesize and characterize fundamental and end-use properties from Nano-particle Cross-linkable latexes and their mixture designs.

Conclusions

This study would be a fundamental and practical contribution to product development at the resin development stage, coatings formulation stage as well as to the final product development and commercialization stage.

The key findings of the study are summarized as follows:

- The study showed that in case of pre-coalescence cross-linked latexes addition of up to 4 mass% of 1,3-BGDMA has a significant effect on increasing the T_g at the 4% level. In case of post-coalescence latexes there is a negligible effect on the T_g at the 5% level.
- The stress–strain behavior, nanoindentation studies and DMA temperature scan profiles showed that in case of post-coalescence cross-linked latexes the properties improve at increasing levels of cross-linking while in case of pre-coalescence cross-linked latexes; very low levels of pre-coalescence cross-linking might improve certain properties. However, as the cross-linker level in pre-coalescence cross-linked latexes increased, the particles were increasingly

resistant to interdiffusion and perhaps to coalescence, resulting in inferior films. On the other hand post-coalescence cross-linked latexes of the type studied here were apparently able to coalesce and interdiffuse sufficiently before the cross-link density was high enough to impede the formation of desirable films.

- With the use of AFM the film formation as a function of time can clearly be seen through evolution of mechanical properties and morphological changes with time for post-coalescence and pre-coalescence cross-linking.

Acknowledgements

This research was supported by the Coatings Research Institute (CRI) and College of Technology (COT) at Eastern Michigan University. This support is greatly appreciated. The authors would especially like to thank Sundaresan Avudaiappan for his help with DMA time-evolution study experiments and Paul Ziemer for his help with the latex polymerization experimental set-up.

References

1 B. Bufkin, J. Coat. Technol., 50 (1978) 41.
2 J. Grawe, J. Coat. Technol., 50 (1978) 67.
3 B. Bufkin, J. Coat. Technol., 50 (1978) 83.
4 J. Grawe, J. Coat. Technol., 50 (1978) 70.
5 B. Bufkin, J. Coat. Technol., 50 (1978) 65.
6 J. W. Taylor and M. A. Winnik, J. Coat. Technol. Res., 1 (2004) 163.
7 M. A. Winnik, J. Coat. Technol., 74 (2004) 49.
8 M. A. Winnik, Polym. Prepr., 44 (2003) 100.
9 M. A. Winnik, P. A. Lovell and M. S. El-Asser, Emulsion Polymerization and Emulsion Polymers, John Wiley and Sons, New York 1997, p. 467.
10 A. Zosel and G. Ley, Macromolecules, 26 (1993) 2222.
11 Y. Huang and F. N. Jones, Prog. Org. Coat., 28 (1996) 133.
12 G. Teng and M. D. Soucek, J. Polym. Sci. Part A: Polym. Chem., 40 (2002) 4256.
13 Technical information sheet, Diacetone acrylamide, N-(1,1-dimethyl-3-oxobutyl)-acrylamide, Kyowa Hakko USA. Inc., p. 4.
14 L. E. Coleman *et al*., J. Polym. Sci. Part A: Polym. Chem., 3 (1965) 1601.
15 U.S.Patent 4,210,565, Ambient or low-temperature curable coatings, 1980.
16 U.S.Patent 4,267,091, Binders for paints, 1981.
17 U.S.Patent Application 20020103278, Waterborne coating compositions, 2002.
18 U.S.Patent 6,605,359, Coating compositions and coatings formed therefrom, 2003.
19 W. Shen, J. Sun, Z. Liu, W. Mao, J. D. Nordstrom, P. D. Ziemer and F. N. Jones, J. Coat. Technol. Res., 1 (2004) 117.
20 M. Song, D. J. Hourston, M. Reading, H. M. Pollock and A. Hammiche, J. Therm. Anal. Cal., 56 (1999) 991.
21 B. Ormsby, G. Foster, T. Learner, S. Ritchie and M. Schilling, J. Therm. Anal. Cal., 90 (2007) 249.
22 B. Ormsby, G. Foster, T. Learner, S. Ritchie and M. Schilling, J. Therm. Anal. Cal., 90 (2007) 503.

DOI: 10.1007/s10973-007-8682-7